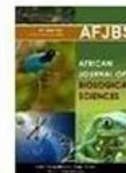


<https://doi.org/10.33472/AFJBS.6.Si2.2024.3712-3728>



African Journal of Biological Sciences

Journal homepage: <http://www.afjbs.com>



Research Paper

Open Access

Assessment of the Bio-enhancing Potential of *Carum Carvi* Extract in Transdermal Drug Delivery Systems for Hypertension

Imran A Sheikh^{1*}, Sachin S. Sakat^{2,3}, Rakesh S. Dhole⁴, Praful G. Rajpurohit⁴, Ashishkumar R. Jadhav³, Hemant S. Mali⁴, Vaishali T. Khairnar⁴, Sandeep S. Pathare⁵

¹Anjuman-I-Islam's Kalsekar Technical Campus, School of Pharmacy, Navi Mumbai- 410206, India

²Department of Pharmacology, Shribios Innovations (OPC) Pvt Ltd, Wagholi, Pune-412207, India

³Shri Ganpati Institute of Pharmaceutical Sciences and Research, Tembhurni, Solapur- 413211, India

⁴Ahinsa Institute of Pharmacy, Dondaicha- 425408, India

⁵Bharati Vidyapeeth (Deemed to be University), Poona College of Pharmacy, Erandwane, Pune- 411038, India

Corresponding Author: Dr. Imran A Sheikh, Associate Professor, Anjuman-I-Islam's Kalsekar Technical Campus, School of Pharmacy, Navi Mumbai- 410206, India
Email ID: iaspharma@gmail.com

Abstract

This study explores the use of *Carum carvi* (caraway) extract to enhance the bioavailability and efficacy of valsartan, an angiotensin II receptor blocker, in transdermal drug delivery systems. Various solvent extracts of *Carum carvi* were incorporated into valsartan-loaded transdermal patches, and their effects were assessed through physicochemical and bioactivity evaluations. Among the extracts, the ethanolic extract (F5) demonstrated the highest bioavailability, with a significant increase in drug absorbance (3.19) and cumulative drug release (CDR) of 66.13%. FTIR analysis confirmed no significant interactions between valsartan and the extracts or polymers. The study concludes that *Carum carvi* extract, particularly in ethanolic form, effectively enhances the transdermal delivery of valsartan, offering valuable insights into the use of phytomedicine and nanotechnology in improving drug delivery systems. These findings suggest potential for better management of chronic conditions like hypertension. Future research should explore the long-term stability and clinical efficacy of these formulations.

Keywords: *Carum carvi*, transdermal drug delivery, valsartan, bioenhancer, nanotechnology, phytomedicine, bioavailability, hypertension, solvent extraction, FTIR analysis.

Article History

Volume 6, Issue Si2, 2024

Received: 29 Apr 2024

Accepted : 30 May 2024

doi: [10.33472/AFJBS.6.Si2.2024.3712-3728](https://doi.org/10.33472/AFJBS.6.Si2.2024.3712-3728)

1. INTRODUCTION

Transdermal drug delivery systems have gained significant attention in the pharmaceutical industry as an alternative to traditional routes of administration. These systems offer numerous advantages, such as the elimination of first-pass metabolism, improved patient compliance, and the potential for prolonged drug administration. One of the key challenges in transdermal drug delivery is enhancing the bioavailability and bioactivity of the active pharmaceutical ingredients (APIs) in the formulation. [1]

Phytomedicine, or plant-derived medicinal compounds, have shown promise in improving the bioavailability and bioactivity of transdermal drug delivery systems. *Carum carvi*, commonly known as caraway, is a plant that has been used in traditional medicine for its various therapeutic properties. [2] *Carum carvi* extract has been investigated for its potential to act as a bioenhancer in transdermal drug delivery systems, potentially improving the absorption and efficacy of the delivered drugs.

Nanotechnology has emerged as an effective tool for enhancing the bioavailability and bioactivity of phytomedicines, including *Carum carvi* extract. Nanomaterial-based

formulations have been shown to improve the solubility, stability, and permeability of plant-derived compounds, leading to enhanced therapeutic outcomes [3] For example, curcumin, a compound found in turmeric, has demonstrated limited efficacy due to its poor bioavailability, but the use of nanomedicine strategies has helped to overcome these challenges and improve its therapeutic potential. [4], [5], [6]

In this research paper, we aim to assess the bioenhancing potential of *Carum carvi* extract in transdermal drug delivery systems. We will evaluate the impact of incorporating *Carum carvi* extract, either in its native form or in a nanoparticle-based formulation, on the bioavailability and bioactivity of the delivered drugs. The findings of this study will contribute to the understanding of the potential of *Carum carvi* extract as a bioenhancer in transdermal drug delivery systems and provide insights into the application of nanotechnology for improving the delivery of drug.

Valsartan

Hypertension, a prevalent global health concern, has been a subject of extensive research and clinical interventions, with the aim of effectively managing this condition and reducing its associated risks. One such pharmacological treatment for hypertension is valsartan, an angiotensin II receptor blocker (ARB) that has gained recognition for its efficacy in managing this chronic condition.

In recent years, several studies have explored the role of valsartan in the management of hypertension. A systematic review by [7] examined the effectiveness of individual interventions, including pharmacological treatment, in improving adherence to prescribed regimens among individuals with primary hypertension. The findings suggest that targeted interventions, such as the use of valsartan, can significantly improve adherence to medication, ultimately contributing to better blood pressure control and improved patient outcomes.

Similarly, a review of the literature on hypertension management published in the last year highlighted the impact of new evidence on various aspects of hypertension, including pharmacological interventions like valsartan. The review discusses the importance of considering real-world data in evaluating the effectiveness of antihypertensive treatments, such as valsartan, in clinical practice. [8]

The effectiveness of valsartan in the management of hypertension has also been explored in the context of multifactorial interventions. A cluster-randomized clinical trial by Banegas et al. investigated the impact of a comprehensive intervention, which included self-management of antihypertensive medication, on blood pressure control among individuals with hypertension. The findings of this study suggest that a multifaceted approach, incorporating pharmacological interventions like valsartan, can enhance adherence and improve overall hypertension management.

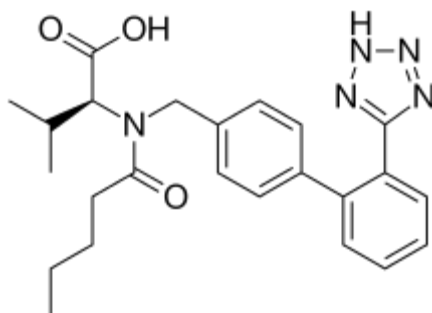


Figure 1 Chemical Structure of Valsartan

Structure of Skin

The skin, the largest organ of the human body, is a complex and intricate structure that serves several critical functions, including protection, sensation, temperature regulation, and immune response. It consists of two main layers, the epidermis and the dermis, each with their own unique characteristics and roles. [9]

The epidermis is the outermost layer of the skin and acts as a barrier against environmental pathogens, regulating the amount of water lost from the body through trans epidermal water loss. [10] Primarily composed of keratinocytes, which produce keratin, the epidermis undergoes continuous renewal as stem cells proliferate and terminally differentiate as they move upward towards the surface. [11]

The dermis, the second layer of the skin, is largely composed of a dense extracellular matrix rich in collagen and elastin, providing the skin with its elasticity and mechanical resistance. This layer also contains blood capillaries, nerve endings, sweat glands, and hair follicles, allowing for functions such as temperature regulation, sensory detection, and immune surveillance. [12] Fibroblasts, the main cellular constituents of the dermis, play a crucial role in the production and maintenance of the extracellular matrix.

The aging process can lead to significant alterations in the dermal extracellular matrix microenvironment, which can impact the skin's protective barrier function and regenerative capacity. Understanding the complex structure and function of the skin is essential for developing effective strategies for skin repair and regeneration, particularly in the context of aging and injury.

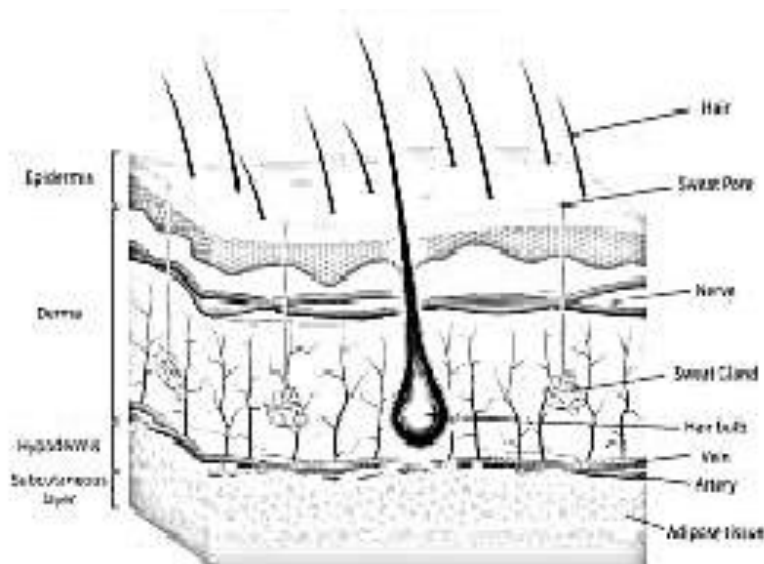


Figure 2 Structure of skin

2. MATERIALS AND METHODS

2.1. Drugs and Chemicals

Valsartan was generously provided by Torrent Pharmaceuticals Ltd. (Gujarat). Additional reagents and chemicals were procured from Research Lab Mumbai. All substances used were of analytical grade.

2.2. Plant Material Used

Carum carvi Fruits were sourced from the local market. Impurities and foreign materials were inspected and removed. The Fruits were authenticated by a plant scientist.

2.1.1 Carum Carvi [13], [14], [15], [16]

Biological Source:

Carum carvi, commonly known as caraway, is a biennial plant in the Apiaceae family. The Fruits used are harvested from mature plants.



Figure 3 a. Carum carvi Plant



3 b. Carum carvi fruits

Chemical Constituents:

Carum carvi Fruits contain a variety of bioactive compounds, including:

Essential oils (2-7%): Carvone (50-60%) and limonene (40-50%)

- Flavonoids
- Phenolic acids
- Fatty acids
- Proteins
- Fiber
- Vitamins and minerals (e.g., vitamin C, iron, calcium)

Uses:

- Carum carvi Fruits are utilized for various purposes, including:
- Culinary: Used as a spice in bread, cakes, and curries for their distinct flavor.
- Medicinal: Traditionally used to treat digestive disorders, such as bloating, gas, and indigestion. They are also known for their antispasmodic, carminative, and antimicrobial properties.
- Cosmetic: Included in skincare formulations for their antioxidant properties.
- Agricultural: Employed as a natural insect repellent in some regions.

2.3 Successive Solvent Extraction

Extraction Methodology of Carum carvi Fruit ¹⁷

Carum carvi fruits were subjected to serial hot extraction using Soxhlet apparatus to identify the extract with the highest bio-enhancing activity. The extraction process was conducted as follows:

- Chloroform
- Butanol
- Methanol
- Ethanol
- Aqueous solution

All materials were air-dried in the shade to obtain a consistent weight. The dried samples were then ground into a coarse powder. Fifty grams of the crude bark powder were placed in the Soxhlet apparatus, and serial extraction was performed with different solvents (chloroform, butanol, methanol, ethanol, and aqueous solution).

The extracts were filtered using a funnel and Whatman No. 1 filter paper. The filtrates were then concentrated to dryness under reduced pressure at 40°C using a rotary evaporator. The dried extracts were stored at 4°C for further studies.

Preparation of Stock Solution and Calibration Curve for Valsartan ¹⁸

A stock solution of Valsartan was prepared using phosphate buffer. This stock solution was subsequently diluted to create a series of standard solutions. The calibration curve was then obtained by measuring the absorbance of these standard solutions at 250 nm wavelength.

Table 1 Standard Curve of Valsartan

| S. No. | Concentration (µg/ml) | Absorbance |
|--------|-----------------------|------------|
| 1 | 5 | 0.166 |
| 2 | 10 | 0.469 |
| 3 | 15 | 0.814 |
| 4 | 20 | 1.100 |
| 5 | 25 | 1.410 |

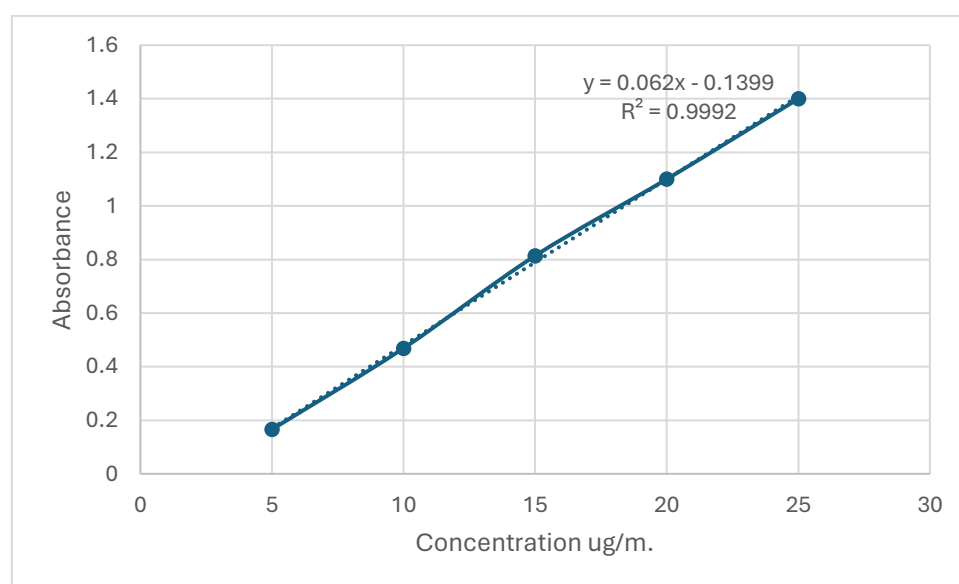


Figure 4 Standard Curve for Valsartan

Formulation and Development of Transdermal Patches

Transdermal patches were applied using a method called soluble solvent casting. Three milliliters of pure water were contained with the precisely weighed HPMC. To allow the compound to swell, the contents of the beaker were mixed for 15 minutes using a magnetic stirrer. Propylene glycol was added to the compound resolution at that time. Two milliliters of water were used to dissolve 100 milligrams of Valsartan. With the use of a magnetic stirrer, the component dispersion and the pharmaceutical arrangement were combined, adding to the citric acid. At that point, after compounding was finished, the resolution could not square for 20 minutes to ensure that all air bubbles had been removed. It was then methodically poured into Petri plates and allowed to dry for a full day at room temperature. Following a 24-hour drying period, patches were removed by removing them from the Petri dishes and dipping a 2-by-2-cm square component at that time. The patches were sealed tightly with foil and stored in an airtight and waterproof container to maintain their dependability and suppleness. [19], [20], [21]

Table 2 Formulation code

| Ingredients | FORMULATION CODE | | | | | |
|--------------------|------------------|------------|------------|------------|------------|------------|
| | F1 | F2 | F3 | F4 | F5 | F6 |
| Valsartan | 40 mg | 40 mg | 40 mg | 40 mg | 40 mg | 40 mg |
| HPMC | 350 mg | 350 mg | 350 mg | 350 mg | 350 mg | 350 mg |
| PG | 0.4 ml | 0.4 ml | 0.4 ml | 0.4 ml | 0.4 ml | 0.4 ml |
| PEG-400 | 0.4 ml | 0.4 ml | 0.4 ml | 0.4 ml | 0.4 ml | 0.4 ml |
| Citric Acid | 20 mg | 20 mg | 20 mg | 20 mg | 20 mg | 20 mg |
| Water | Up to 5 ml | Up to 5 ml | Up to 5 ml | Up to 5 ml | Up to 5 ml | Up to 5 ml |
| Chloroform extract | ----- | 50 mg | ----- | ----- | ----- | ----- |
| Butanolic Extract | ----- | ----- | 50 mg | ----- | ----- | ----- |
| Methanolic Extract | ----- | ----- | ----- | 50 mg | ----- | ----- |
| Ethanolic Extract | ----- | ----- | ----- | ----- | 50 mg | ----- |
| Aqueous extract | ----- | ----- | ----- | ----- | ----- | 50 mg |

Evaluation of Transdermal Delivery Patches:

Transdermal patches were evaluated physiochemically using the following parameters.

A certain section of the film was dissolved in a phosphate buffer solution, indicating the presence of drugs. The transdermal patch was dissolved by stirring the fluid. The contents are transferred to a volumetric flask.

The drug's content material was ascertained by measuring the change in absorbance of the solution

a. Material percentage moisture content: The prepared patches were weighed individually and kept for 24 hours at room temperature in a desiccator filled with fuse calcium chloride. The

patches were weighed after a 24-hour period, and the fraction of moisture content material was determined [22].

c. Folding endurance: A piece of film that is cut uniformly and repeatedly folded at the same spot until it breaks. Given the estimated folding endurance, the number of times the film was distorted in a same area without breaking [23].

d. Weight uniformity: Films with a diameter of 4 cm and a radius of 2 cm were cut. The weight discrepancy was intended, and the masses of five films were taken [24].

e. Moisture uptake percentage: To maintain an 84% relative humidity, the weighed patches were kept in desiccators at room temperature for a full day. The patches were saturated with potassium chloride.

The patches were reweighed after a 24-hour period in order to calculate the formula's moisture uptake percentage [22].

f. Patch thickness: Using screw gauze at five different locations on the film, the thickness of each transdermal patch was measured, and the mean value was found [23].

Table 3 Evaluation of the Formulated Transdermal patches

| FORMULATION CODE | | | | | | |
|------------------------|-------------|-------------|-------------|-------------|-------------|-------------|
| Parameters | F1 | F2 | F3 | F4 | F5 | F6 |
| Thickness (mm) | 0.245±0.015 | 0.226±0.017 | 0.220±0.021 | 0.311±0.009 | 0.322±0.014 | 0.346±0.016 |
| Weight uniformity (gm) | 0.321±0.016 | 0.225±0.015 | 0.255±0.027 | 0.231±0.013 | 0.129±0.025 | 0.121±0.017 |
| % Moisture uptake | 9.112±2.124 | 8.123±3.004 | 9.225±1.213 | 8.234±2.312 | 9.121±2.454 | 8.212±2.321 |
| % Moisture content | 4.342±0.766 | 7.128±0.673 | 6.121±0.342 | 6.230±0.774 | 8.216±0.312 | 6.221±0.876 |
| % Drug content (mg) | 79.1±0.233 | 87.45±0.563 | 77.45±0.459 | 79.33±0.243 | 81.70±0.780 | 83.11±0.991 |
| Folding Endurance | 26±2.77 | 33±5.23 | 27±4.56 | 31±3.65 | 32±2.34 | 32±4.80 |

*All data are presented in Average ± SD, n=3

Bio enhancing Activity Model:

B. Franz Diffusion Cell:

The goatskin that was obtained was appropriately preserved in phosphate buffer for the ex-vivo permeation research. Franz diffusion cells with an effective sectional area of 3.14 cm² and 15 ml of receiver chamber potential were used to conduct ex vivo permeation studies. The goatskin that has been treated shrinks to the ideal size and is positioned between the diffusion cell's donor and receptor compartments.

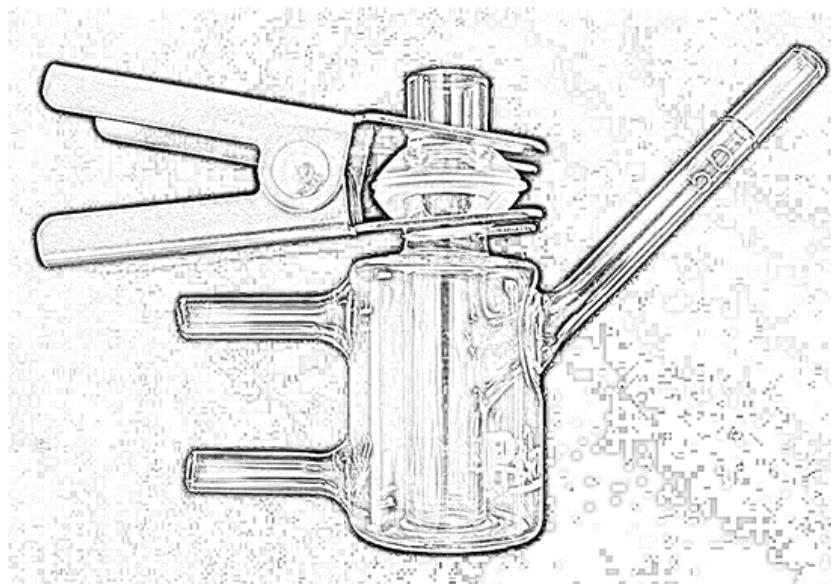


Figure 5 Franz Diffusion Cell

The membrane is covered by the patch. The donor compartment is positioned above the receptor compartment, which is filled with phosphate buffer (pH 7.4) and kept at $37 \pm 0.5^\circ\text{C}$. A clamp is positioned over the donor and receptor compartments to secure them together, and the entire assembly is placed on a magnetic stirrer. With magnetic beads, the contents of the receiver compartment were continuously agitated. During scheduled time intervals, the unique quantity of the pattern was substituted with an equal amount of phosphate buffer, hence determining the amount of medicine injected through the membrane. With the help of a spectrophotometer, the samples' absorbance becomes fascinating [24], [25], [26].

Table 4 % CDR of Carum carvi Fruit extracts + Valsartan patches

| Time in hrs. | F1 | F2 | F3 | F4 | F5 | F6 |
|--------------|------------|------------|------------|------------|------------|------------|
| 0.5 | 1.50±0.77 | 2.50±0.46 | 3.50±0.53 | 4.50±0.41 | 6.00±0.43 | 1.90±0.60 |
| 1.0 | 2.75±0.53 | 3.28±0.66 | 4.28±0.76 | 5.65±0.42 | 8.54±0.55 | 3.46±0.36 |
| 1.5 | 5.60±1.76 | 5.95±0.65 | 6.95±0.22 | 7.58±0.65 | 9.56±1.77 | 5.80±0.55 |
| 2.0 | 7.50±1.61 | 9.50±1.77 | 11.78±0.54 | 12.11±1.37 | 14.12±1.33 | 8.67±1.86 |
| 2.5 | 9.23±0.67 | 12.34±1.45 | 14.32±1.49 | 16.54±1.86 | 19.45±0.66 | 10.45±1.67 |
| 3.0 | 10.55±1.62 | 16.66±1.44 | 19.67±1.64 | 22.23±1.75 | 25.12±0.75 | 12.88±1.75 |
| 4.0 | 13.67±1.77 | 22.88±0.55 | 25.56±1.66 | 28.47±0.47 | 33.34±1.66 | 15.78±1.66 |
| 5.0 | 20.50±1.43 | 30.72±0.54 | 33.45±1.97 | 36.43±1.97 | 39.45±1.12 | 25.22±1.35 |
| 6.0 | 32.15±0.72 | 41.26±0.81 | 48.12±0.57 | 50.12±1.55 | 54.11±1.33 | 35.56±0.66 |
| 8.0 | 50.30±1.77 | 50.52±1.57 | 56.67±0.25 | 63.56±0.66 | 66.13±1.21 | 53.89±1.76 |

*All data are presented in Average \pm SD, n=3

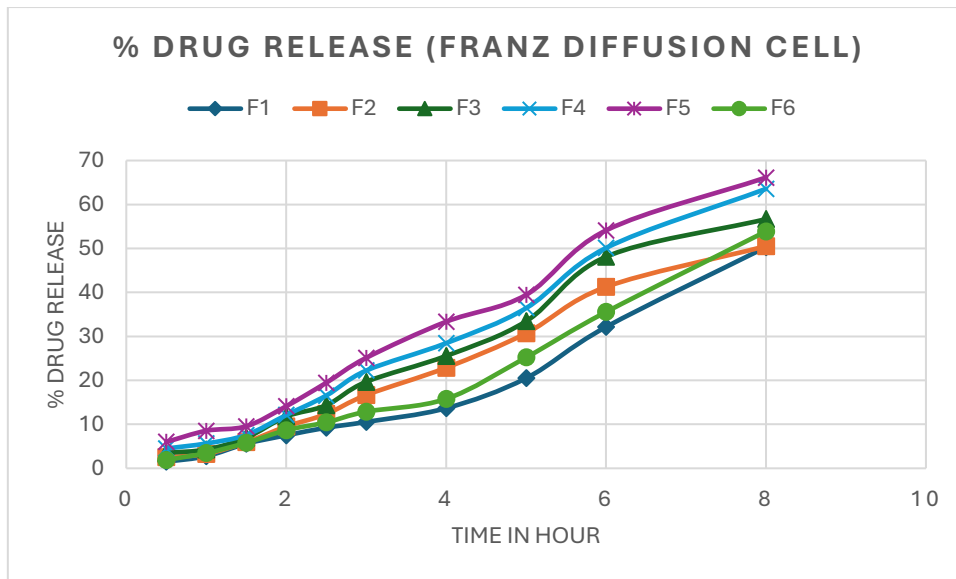


Figure 6 % Drug Release Franz Diffusion cell

B. Everted GUT Sac Model

tiny intestine was purchased from local markets that housed slaughterhouses. The intestinal segment was collected in two 15-cm sections after being carried in a buffer solution; the estimated intestinal diameter was 0.07 cm. A tumbler rod was used to tie up and evert one end of the gut; the cannula was connected to another end of the intestine to allow for the shaping of the pouch and the delivery of a tiny amount of drug-free buffer solution.

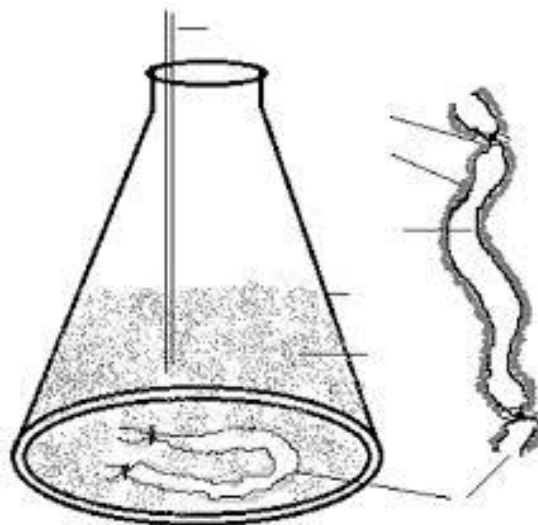


Figure 7 Everted Gut Sac Model

With the use of an oxygen pump and phosphate buffer solution, the tissue was continuously supplied with oxygen to keep it alive; the temperature remained constant at $37 \pm 0.5^\circ\text{C}$ throughout the process. Following eversion, the serosal facet was visible inside and the mucosal side emerged. The skin's stratum corneum side became in close proximity to the transdermal patch's releasing surface. The pattern from the sac is withdrawn at a predetermined period, and a spectrophotometer is used to detect the drug's concentration in a serosal fluid. Ultimately, the absorbance percentage is computed against time [27] [28] [29].

Table 5 %Drug absorbed of Carum carvi Fruit extract Valsartan bulk drug

| Time in Min. | F1 | F2 | F3 | F4 | F5 | F6 |
|--------------|------------|------------|------------|------------|------------|------------|
| 10 | 0.450±0.31 | 0.500±0.61 | 0.710±0.24 | 0.742±0.55 | 1.047±0.87 | 0.460±0.57 |
| 20 | 0.798±0.52 | 0.848±0.33 | 0.914±0.35 | 1.054±0.41 | 1.424±0.61 | 0.800±0.71 |
| 30 | 1.144±0.82 | 1.212±0.47 | 1.302±1.24 | 1.641±0.47 | 1.821±0.54 | 1.112±0.42 |
| 60 | 1.312±0.42 | 1.387±0.65 | 1.505±1.31 | 1.878±0.39 | 2.205±0.53 | 1.320±0.67 |
| 90 | 1.642±0.92 | 1.820±0.65 | 2.007±1.45 | 2.350±0.94 | 2.751±0.61 | 1.749±0.49 |
| 120 | 2.074±0.27 | 2.204±0.31 | 2.310±0.84 | 2.720±1.01 | 3.194±0.38 | 2.282±0.71 |

*All data are presented in Average ± SD, n=3

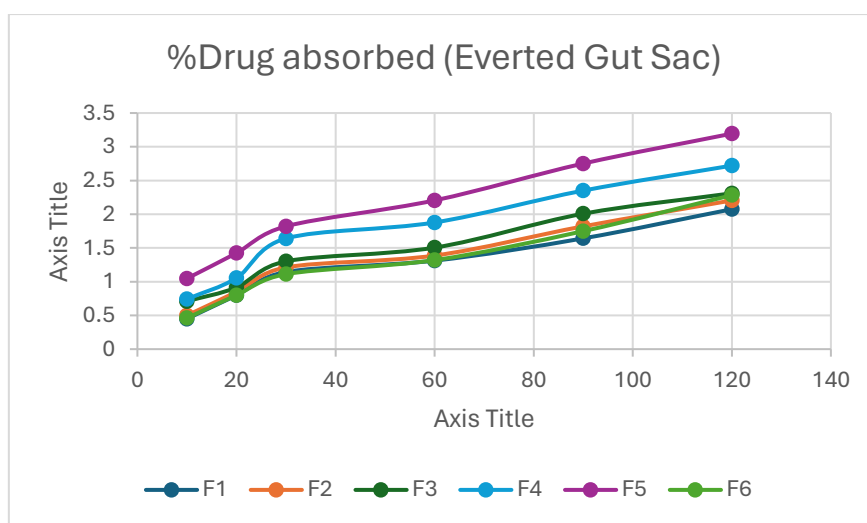


Figure 8 % Drug absorbed of Carum carvi fruit Extracts + Valsartan bulk drug

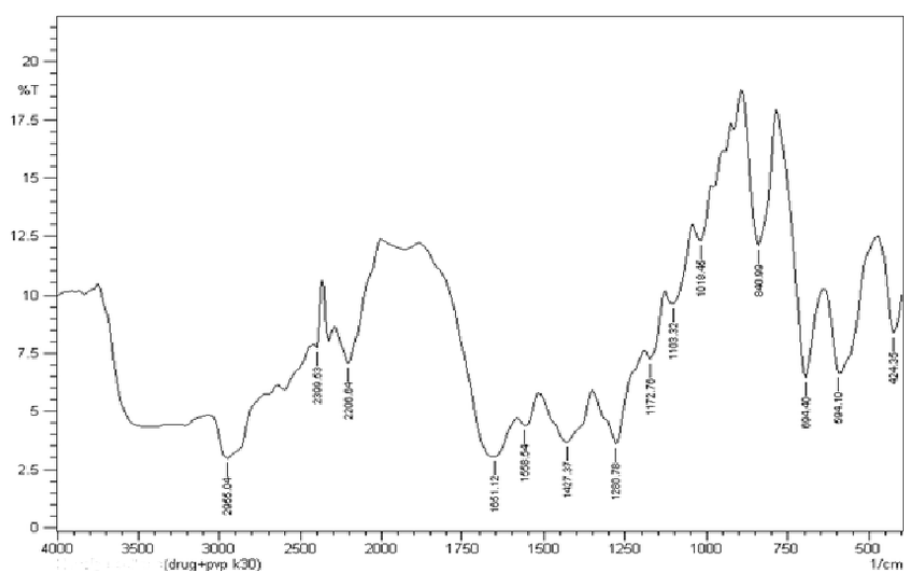


Figure 9 FTIR of Pure Valsartan

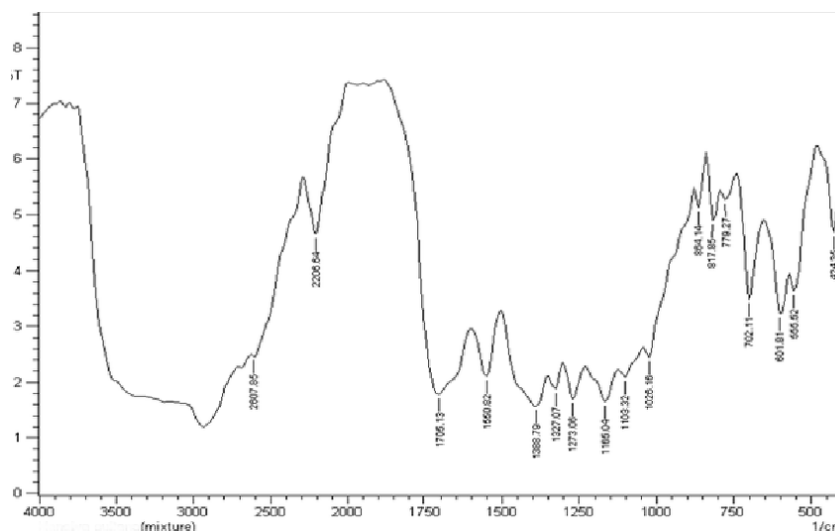


Figure 10 FTIR with Physical mixture of Carum carvi Ethanolic Extract (F5)

FTIR Spectrum of Valsartan

Valsartan is an angiotensin II receptor blocker used to treat high blood pressure. The key functional groups in Valsartan and their corresponding absorption bands in the FTIR spectrum are as follows:

N-H Stretch (Amine):

Region: 3300-3500 cm^{-1}

Typical Absorption: Broad band, often indicating the presence of primary or secondary amines.

C=O Stretch (Carboxylic Acid or Amide):

Region: 1650-1750 cm^{-1}

Typical Absorption: Strong, sharp peak due to the carbonyl group.

C=C Stretch (Aromatic Ring):

Region: 1450-1600 cm^{-1}

Typical Absorption: Multiple peaks, indicative of aromatic rings.

C-N Stretch (Amine):

Region: 1200-1350 cm^{-1}

Typical Absorption: Medium peaks due to the stretching vibrations of the C-N bonds.

O-H Stretch (Carboxylic Acid):

Region: 2500-3300 cm^{-1}

Typical Absorption: Broad, overlapping with N-H stretch if present.

FTIR Spectrum of Valsartan plus Carum carvi Ethanolic Extract

When Valsartan is combined with Carum carvi (caraway) ethanolic extract, the FTIR spectrum will show additional absorption bands due to the components of the extract. Carum carvi contains several bioactive compounds such as carvone, limonene, and flavonoids, which contribute to the following bands:

O-H Stretch (Phenolic Compounds and Alcohols):

Region: 3200-3600 cm^{-1}

Typical Absorption: Broad band indicating the presence of hydroxyl groups.

C=O Stretch (Ketones, Aldehydes, and Esters):

Region: 1700-1750 cm^{-1}

Typical Absorption: Strong, sharp peak for carbonyl groups present in components like carvone.

C-H Stretch (Alkanes and Aromatic Compounds):

Region: 2800-3000 cm^{-1}

Typical Absorption: Multiple peaks representing various C-H stretching vibrations.

C=C Stretch (Alkenes and Aromatics):

Region: 1600-1680 cm^{-1}

Typical Absorption: Strong peaks for aromatic rings and alkenes.

C-O Stretch (Alcohols, Ethers, and Esters):

Region: 1050-1300 cm^{-1}

Typical Absorption: Strong peaks indicating the presence of C-O bonds.

Comparative Interpretation

Shift in Absorption Bands:

Compare the spectra of pure Valsartan with that of the Valsartan-Carum carvi mixture. Any shifts in the absorption bands can indicate interactions between Valsartan and the compounds in the extract.

New Absorption Bands:

Look for new absorption bands in the Valsartan-Carum carvi spectrum that are not present in the pure Valsartan spectrum. These bands correspond to functional groups in the Carum carvi extract.

Intensity Changes:

Observe changes in the intensity of the absorption bands. Increased or decreased intensity can indicate changes in the concentration of specific functional groups due to interactions between the drug and the extract.

Disappearance of Bands:

If any characteristic bands of Valsartan are missing in the combination spectrum, it might suggest the formation of new compounds or complexes.

3. RESULT AND DISCUSSION

The patches that were correctly formulated underwent diffusion analysis, which was facilitated by the utilization of the Franz diffusion cellular method and the inverted intestinal sac. In order to ascertain the percentage of drug content, samples were taken at a prearranged time, and each sample's absorbance was evaluated using a spectrophotometer. The graph illustrates the outcome of the diffusion research by graphing time on the x-axis, cumulative percentage release on the y-axis, and percentage absorbance against time in the case of the everted intestinal sac model. This study has shown that using natural bioenhancers, such as Carum carvi Fruit extract, in conjunction with contemporary medications, such as Valsartan can increase the drug's bioavailability when administered via transdermal drug delivery device.

The patches that were correctly formulated underwent diffusion analysis, which was facilitated by the utilization of the Franz diffusion cellular method and the inverted intestinal sac. Samples were gathered at a prearranged time, and each sample's absorbance was analyzed using a spectrophotometer to ascertain the percentage of drug content. The graph illustrates the outcome of the diffusion research by graphing time on the x-axis, cumulative percentage release on the y-axis, and percentage absorbance against time in the case of the everted intestinal sac model. This study has shown that using natural bioenhancers, such as Carum

carvi Fruit extract, in conjunction with contemporary medications, such as Valsartan, can increase the drug's bioavailability when administered via transdermal drug delivery device. With the aid of FTIR, compatibility investigations between drugs and extracts as well as drugs and polymers reveal no interactions between drugs and extracts or between drugs and polymers, as shown by the results.

physicochemical characteristics, such as thickness, weight version, percentage moisture content, and so forth. Franz Diffusion cell studies are mentioned in Table 4 and Figure 6, while everted intestinal sac studies are mentioned in Table 5 and Figure 8. of all the extracts, ethanolic extract (F5) demonstrated a significant increase in both drug absorbance (3.19) and % CDR 66.13. These results are within the range shown in Table 4. Study on the Order of Permeation Enhancing Effect Franz Diffusion Cell

Drug absorption percentage order in the case of an everted intestinal sac model:
F5>F4>F3>F2>F6>F1

Long-term treatment and multidrug therapy may be successfully completed with the use of a transdermal drug delivery device, which will also boost the medication's bioavailability by preventing first-pass metabolism, which would otherwise destroy the drug's maximal amount. The medication immediately enters the systemic flow and improves the effectiveness of healing. A potent anti-diabetic medication called Valsartan is widely used to treat type-ii diabetes. However, the primary-skip metabolism suggests that the therapeutic impact is diminished. Polymers were chosen, together with HPMC, since they verified proper adhesive activity and increased skeleton formation, which forms the basis of transdermal patches. Phosphate buffer 7.4, which was utilized to determine the drug's unknown concentration and assess the drug's solubility There was no drug-drug or drug-polymer interaction, according to FTIR measurements. To standardize the formulation, the prepared patches were put through a series of physical and chemical evaluation criteria. Every parameter that has been assessed for different components is subject to limitations.

Formulation F5 demonstrated the highest bioavailability of Valsartan among all the components when compared to other extracts.

By comparing the FTIR spectra of Valsartan and the Valsartan plus Carum carvi ethanolic extract, you can identify the functional groups involved in any interactions, detect the presence of new compounds, and understand the chemical environment changes in the mixture. This interpretation helps in understanding the compatibility and potential synergistic effects of the combined formulation.

References:

1. Ghalandarlaki, N., Alizadeh, A M., & Ashkani-Esfahani, S. (2014, January 1). Nanotechnology-Applied Curcumin for Different Diseases Therapy. Hindawi Publishing Corporation, 2014, 1-23. <https://doi.org/10.1155/2014/394264>
2. Gunasekaran, T., Haile, T., Nigusse, T., & Dhanaraju, M D. (2014, May 1). Nanotechnology: an effective tool for enhancing bioavailability and bioactivity of phytomedicine. Medknow, 4, S1-S7. <https://doi.org/10.12980/apjtb.4.2014c980>
3. Pandey, R K., Bhairam, M., Shukla, S S., & Gidwani, B. (2021, July 29). Colloidal and vesicular delivery system for herbal bioactive constituents. Springer Nature, 29(2), 415-438. <https://doi.org/10.1007/s40199-021-00403-x>

4. Patra, J K., Das, G., Fraceto, L F., Campos, E V R., Rodríguez-Torres, M D P., Acosta-Torres, L S., Díaz-Torres, L., Grillo, R., Swamy, M K., Sharma, S., Habtemariam, S., & Shin, H S. (2018, September 19). Nano based drug delivery systems: recent developments and future prospects. *BioMed Central*, 16(1). <https://doi.org/10.1186/s12951-018-0392-8>
5. Yallapu, M M., Jaggi, M., & Chauhan, S C. (2013, April 1). *Curcumin Nanomedicine: A Road to Cancer Therapeutics*. Bentham Science Publishers, 19(11), 1994-2010. <https://doi.org/10.2174/138161213805289219>
6. Edwards, E., & DiPette, D J. (2019, April 13). "Real-world data analysis" in disease management such as hypertension: Has the time come?. *Wiley-Blackwell*, 21(5), 635-637. <https://doi.org/10.1111/jch.13533>
7. Parra, D I., Gimeno, I T., Rodríguez, J M S., Corredor, L C R., Vargas, J A H., Romero, L A L., López, F J G., Gómez, C E., Trujillo-Cáceres, S J., Serrano-Gallardo, P., & Vera-Cala, L M. (2020, December 1). Individual interventions to improve adherence to pharmaceutical treatment, diet and physical activity among adults with primary hypertension. A systematic review protocol. *BMJ*, 10(12), e037920-e037920. <https://doi.org/10.1136/bmjopen-2020-037920>
8. A single-cell transcriptome atlas of pig skin characterizes anatomical positional heterogeneity. (2023, June 5). <https://pubmed.ncbi.nlm.nih.gov/37276016>
9. Dove Medical Press - Open Access Publisher of Medical Journals. (2015, February 9). <https://www.dovepress.com/articles.php>
10. Dussoyer, M., Michopoulou, A., & Rousselle, P. (2020, May 15). Decellularized Scaffolds for Skin Repair and Regeneration. *Multidisciplinary Digital Publishing Institute*, 10(10), 3435-3435. <https://doi.org/10.3390/app10103435>
11. Bonlawar, J., Setia, A., Challa, R.R., Vallamkonda, B., Mehata, A.K., Vaishali, , Viswanadh, M.K., Muthu, M.S. (2024). Targeted Nanotheranostics: Integration of Preclinical MRI and CT in the Molecular Imaging and Therapy of Advanced Diseases. *Nanotheranostics*, 8(3), 401-426. <https://doi.org/10.7150/ntno.95791>.
12. Pasala, P. K., Rudrapal, M., Challa, R. R., Ahmad, S. F., Vallamkonda, B., & R., R. B. (2024). Anti-Parkinson potential of hesperetin nanoparticles: in vivo and in silico investigations. *Natural Product Research*, 1–10. <https://doi.org/10.1080/14786419.2024.2344740>
13. Suseela, M. N. L., Mehata, A. K., Vallamkonda, B., Gokul, P., Pradhan, A., Pandey, J., ... & Muthu, M. S. (2024). Comparative Evaluation of Liquid-Liquid Extraction and Nanosorbent Extraction for HPLC-PDA Analysis of Cabazitaxel from Rat Plasma. *Journal of Pharmaceutical and Biomedical Analysis*, 116149. <https://doi.org/10.1016/j.jpba.2024.116149>
14. Chakravarthy, P.S.A., Popli, P., Challa, R.R. et al. Bile salts: unlocking the potential as bio-surfactant for enhanced drug absorption. *J Nanopart Res* 26, 76 (2024). <https://doi.org/10.1007/s11051-024-05985-6>
15. Setia, A., Vallamkonda, B., Challa, R.R., Mehata, A.K., Badgujar, P., Muthu, M.S. (2024). Herbal Theranostics: Controlled, Targeted Delivery and Imaging of Herbal Molecules. *Nanotheranostics*, 8(3), 344-379. <https://doi.org/10.7150/ntno.94987>.

16. Dhamija P, Mehata AK, Tamang R, Bonlawar J, Vaishali, Malik AK, Setia A, Kumar S, Challa RR, Koch B, Muthu MS. Redox-Sensitive Poly(lactic-co-glycolic acid) Nanoparticles of Palbociclib: Development, Ultrasound/Photoacoustic Imaging, and Smart Breast Cancer Therapy. *Mol Pharm.* 2024 May 5. doi: 10.1021/acs.molpharmaceut.3c01086. Epub ahead of print. PMID: 38706253.
17. Eranti, Bhargav and Mohammed, Nawaz and Singh, Udit Narayan and Peraman, Ramalingam and Challa, Ranadheer Reddy and Vallamkonda, Bhaskar and Ahmad, Sheikh F. and DSNBK, Prasanth and Pasala, Praveen Kumar and Rudrapal, Mithun, A Central Composite Design-Based Targeted Quercetin Nanoliposomal Formulation: Optimization and Cytotoxic Studies on MCF-7 Breast Cancer Cell Lines. Available at SSRN: <https://ssrn.com/abstract=4840349> or <http://dx.doi.org/10.2139/ssrn.4840349>
18. Setia A, Challa RR, Vallamkonda B, Satti P, Mehata AK, Priya V, Kumar S, Muthu MS. Nanomedicine And Nanotheranostics: Special Focus on Imaging of Anticancer Drugs Induced Cardiac Toxicity. *Nanotheranostics* 2024; 8(4):473-496. doi:10.7150/ntno.96846. <https://www.ntno.org/v08p0473.htm>
19. Pawankumar Yadav, Saurabh Mishra. Transdermal patch of an Antihypertensive Drug: it's development and Evaluation. *World Journal of Pharmaceutical Research* 2017; 6, 1355-74.
20. S.J Shankar., Palak Kapadiya, Makaranda Prabhu, Prathan Raju. Formulation and Evaluation of Transdermal Patches of An Antidiabetic Drug of Glibenclamide. *World Journal of Pharmacy and Pharmaceutical Sciences* 2015; 5, 522-41.
21. A. Srilakshmi, Ravi Teja, K. Lakshmi, M. Thippesh, SK Ummehani, and B. Salma. Formulation and evaluation of transdermal patches of Irbesartan. *Indian Journal of Research in Pharmacy and Biotechnology* 2017; 5, 212-15.
22. Pawankumar Yadav, Saurabh Mishra. Transdermal patch of an Antihypertensive Drug: it's development and Evaluation. *World Journal of Pharmaceutical Research* 2017; 6, 1355-74.
23. Bhandari S, Chauhan B, Gupta N, et al. Translational Implications of Neuronal Dopamine D3 Receptors for Preclinical Research and Cns Disorders. *African J Biol Sci (South Africa)*. 2024;6(8):128-140. doi:10.33472/AFJBS.6.8.2024.128-140
24. Tripathi A, Gupta N, Chauhan B, et al. Investigation of the structural and functional properties of starch-g-poly (acrylic acid) hydrogels reinforced with cellulose nanofibers for cu²⁺ ion adsorption. *African J Biol Sci (South Africa)*. 2024;6(8): 144-153, doi:10.33472/AFJBS.6.8.2024.141-153
25. Sharma R, Kar NR, Ahmad M, et al. Exploring the molecular dynamics of ethyl alcohol: Development of a comprehensive model for understanding its behavior in various environments. *Community Pract.* 2024;21(05):1812-1826. doi:10.5281/zenodo.11399708
26. Mandal S, Kar NR, Jain AV, Yadav P. Natural Products As Sources of Drug Discovery: Exploration, Optimisation, and Translation Into Clinical Practice. *African J Biol Sci (South Africa)*. 2024;6(9):2486-2504. doi:10.33472/AFJBS.6.9.2024.2486-2504
27. Kumar S, Mandal S, Priya N, et al. Modeling the synthesis and kinetics of Ferrous Sulfate production: Towards Sustainable Manufacturing Processes. *African J Biol Sci (South Africa)*. 2024;6(9):2444-2458. doi:10.33472/AFJBS.6.9.2024.

28. Revadigar RV, Keshamma E, Ahmad M, et al. Antioxidant Potential of Pyrazolines Synthesized Via Green Chemistry Methods. *African J Biol Sci (South Africa)*. 2024;6(10):112-125. doi:10.33472/AFJBS.6.10.2024.112-125
29. Sahoo S, Gupta S, Chakraborty S, et al. Designing, Synthesizing, and Assessing the Biological Activity of Innovative Thiazolidinedione Derivatives With Dual Functionality. *African J Biol Sci (South Africa)*. 2024;6(10):97-111. doi:10.33472/AFJBS.6.10.2024.97-111
30. Binit Patel, Pravinkumar Darji, Arpan Chudasama, Praneeth Ivan Joel Fnu, Seshadri Nalla. Preparation, characterization, and evaluation of a novel co-processed excipient as a directly compressible vehicle in antihypertensive tablet formulation. *Journal of chemical health risks*, volume 14(2), 1711-1717.